JOURNAL OF AGRICULTURAL AND FOOD CHEMISTRY

Article

pubs.acs.org/JAFC

Rosé Wine Fining Using Polyvinylpolypyrrolidone: Colorimetry, Targeted Polyphenomics, and Molecular Dynamics Simulations

Mélodie Gil,[†] Fabian Avila-Salas,[‡] Leonardo S. Santos,[§] Néréa Iturmendi,[∥] Virginie Moine,[∥] Véronique Cheynier,[⊥] and Cédric Saucier*[,†]

[†]SPO, Univ Montpellier, INRA, Montpellier SupAgro, Montpellier, France

[‡]Center for Bioinformatics and Molecular Simulation, Faculty of Engineering, and [§]Laboratory of Asymmetric Synthesis, Institute of Chemistry and Natural Resources, Universidad de Talca, Talca, Chile

[∥]Biolaffort, 126 Quai de la Souys, 33100 Bordeaux, France

[⊥]SPO, INRA, Montpellier SupAgro, Univ Montpellier, Plateforme Polyphénols, Montpellier, France

Supporting Information

ABSTRACT: Polyvinylpolypyrrolidone (PVPP) is a fining agent polymer used in winemaking to adjust rosé wine color and to prevent organoleptic degradations by reducing polyphenol content. The impact of this polymer on color parameters and polyphenols of rosé wines was investigated, and the binding specificity of polyphenols toward PVPP was determined. Color measured by colorimetry decreased after treatment, thus confirming the adsorption of anthocyanins and other pigments. Phenolic composition was determined before and after fining by targeted polyphenomics (UPLC-electrospray ionization source (ESI)-mass spectrometry (MS)/MS). MS analysis showed adsorption differences among polyphenol families. Flavonols (42%) and flavanols (64%) were the most affected. Anthocyanins were not strongly adsorbed on average (12%), but a specific adsorption of coumaroylated anthocyanins was observed (37%). Intermolecular interactions were also studied using molecular dynamics simulations. Relative adsorptions of flavanols were correlated with the calculated interaction energies. The specific affinity of coumaroylated anthocyanins toward PVPP was also well explained by the molecular modeling.

KEYWORDS: *rosé wine, PVPP, phenolic compounds, CIELAB, interaction energy, molecular dynamics simulations*

INTRODUCTION

Polyphenols are essential molecules found in rosé wines. They can be divided into seven families: benzoic acids, hydroxycinnamic acids, stilbenes, flavonols, flavan-3-ols, dihydroflavonols, and anthocyanins. Their quantities vary depending on different factors such as grape variety, geographic origin, and winemaking process. In wine, they are responsible for quality and sensorial characteristics such as taste and color. More specifically, anthocyanins, which are the red grape pigments, play an important role in wine color.[1] Polyphenols in rosé wines in the presence of SO_2 can also enhance the antioxidant effect of these wines by a synergistic effect.[2] However, an excess of polyphenols may induce defaults like browning problems due to oxidation of polyphenols and especially flavanols.[3−5] During storage, the stability of the pink color of rosé wines may be an issue as more orange pigments may form because of reactions of phenolic acids, flavanols, and anthocyanins, like xanthylium derivatives[6,7] or pyranoanthocyanins, one of the most important classes of anthocyanins derivatives.[8−10] Some thiol aroma compounds may also be trapped by quinones during the oxidative process involved in rosé wine aging.[11] One way to limit these problems is to reduce the polyphenol quantities in the wine using fining agents such as polyvinylpolypyrrolidone (PVPP), a cross-linked synthetic polymer of polyvinylpyrrolidone (PVP) (Figure 1) known to have polyphenol binding affinities. During fining, PVPP adsorbs some polyphenols thus reducing their amounts in alcoholic beverages like beer and wine.[12−14] This adsorption of polyphenols by PVPP involves H-bonding between the proton donor from the polyphenol and the carbonyl group from PVPP, together with polar π-bond overlap (delocalized electrons) and hydrophobic reactions.[15,16] In rosé wine production, PVPP is regularly used to reduce color and phenolics. This fining treatment can be done at the grape must, fermentation, or finished wine stages. In this paper, we chose to focus on the PVPP treatment at the finished wine stage. The aim of this work was to investigate the effect of PVPP on rosé wine color adjustment and the selective polyphenol adsorption phenomenon induced by the treatment in a laboratory-standardized protocol. To achieve this, we used a targeted polyphenomics methodology, which is a metabolomics approach focused on polyphenols, recently developed to measure up to 152 phenolic compounds in rosé wines by using liquid chromatography (LC)-mass spectrometry (MS)/MS in multiple reaction

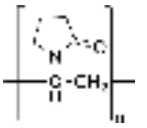

Figure 1. Chemical structure of PVP, $(C_6H_9NO)n$.

Received: September 25, 2017
Revised: November 8, 2017
Accepted: November 8, 2017
Published: November 8, 2017

DOI: 10.1021/acs.jafc.7b04461
J. Agric. Food Chem. XXXX, XXX, XXX−XXX

monitoring (MRM) mode.[17] In addition, interaction energy calculations (at semiempirical quantum mechanical level) and molecular dynamics simulations including dynamic docking were carried out to provide deeper insights into the behavior of the PVPP polymer in a simulated rosé wine solution (ethanol/water). These studies allowed a better understanding of the interactions that govern the PVPP-polyphenols affinity during PVPP treatments on wines.

MATERIALS AND METHODS

Chemicals. All chemicals were of analytical reagent grade. Methanol and formic acid were purchased from Sigma-Aldrich (Saint-Quentin Fallavier, France). Deionized water was obtained from a Milli-Q Advantage A10 purification system from Millipore (Fontenay sous Bois, France). PVPP VINICLAR was obtained from Laffort (Bordeaux, France).

Wines and Sample Preparation. Commercial rosé wines from the same vintage (2015) and from different regions of France were selected (n = 6): Gascogne (1), Languedoc (3), Provence (1), Roussillon (1). A standardized laboratory protocol was developed to allow comparison of a PVPP treatment on rosé wines: a 100 g/L stock solution of PVPP VINICLAR was prepared. After an hour of rest time, 15 mL of wine was supplemented with 120 μL of the PVPP stock solution (final concentration of PVPP = 80 g/hL = maximum legal use). Samples were mixed for 30 s with a vortex and then were left to stand for 1 h at constant room temperature (20 °C) and then were centrifuged at 10 016g (8500 rpm) for 5 min. Initial tests were performed to determine the minimal contact time needed to reach the equilibrium (Appendix 1 of the SI). The supernatant was submitted to spectrophotometric analysis, then was aliquoted in 1.5 mL Eppendorfs, and was stored at −80 °C until further analyses. For mass spectrometry analyses, samples were brought back to ambient temperature, were filtered through a 0.2 μm regenerated cellulose membrane syringe filter (Phenex, Phenomenex, Le Pecq, France), and then were injected with no further sample preparation. Controls went through the same steps but without PVPP addition.

Spectrophotometric L*a*b* Measurements. Color analyses were performed on a spectrophotometer CM-3600d from KONICA MINOLTA with a 1.0 cm length glass cell, between 360 and 740 nm with 10 nm pitch, and were piloted with the SpectraMagic NX software. The CIELAB coordinates L*, a*, b*, h, and C* were obtained using the D65 illuminant and a 10° observer. The CIELAB is a color space defined in 1976.[18] In this three-dimension system, the L* axis indicates that the lightness has a value that extends from 0 (black) to 100 (white); the a* and b* axes represent the chromaticity. Coordinate a* has positive values for red colors and negative values for green colors. Coordinate b* has positive values for yellow colors and negative values for blue colors. L*, a*, and b* form a rectangular coordinate, but any point in this color space can also be defined by the cylindrical coordinates L*, C*, and h. C* and h, respectively, represent chroma and hue angle and are, respectively, calculated as $\sqrt{[(a^*)^2 + (b^*)^2]}$ and $[\arctan(b^*/a^*)]$.[19,20] The difference of colors ΔE between two samples may be calculated as $\sqrt{[(L_1^* - L_2)^2 + (a_1^* - a_2^*)^2 + (b_1^* - b_2^*)^2]}$; if this value is superior to 1, a color difference can be perceived by the human eye, and the bigger the ΔE value, the easier it is to notice the color difference.[21]

UPLC-QqQ-MS Parameters. Polyphenol analyses were performed with a Waters Acquity UPLC system connected to a triple quadrupole mass spectrometer equipped with an electrospray ionization source (ESI) operating in switching positive and negative mode. The UPLC system included a binary pump, a cooled autosampler maintained at 7 °C and equipped with a 5 μL sample loop, a 100 μL syringe and a 30 μL needle, a thermostated column department, and a DAD detector. MassLynx software was used for instrument control and data acquisition, and then TargetLynx software was used for data processing. Quantitative analyses were performed by UHPLC-QqQ-MS using the multiple reaction monitoring (MRM) detection mode under the conditions (high-performance liquid chromatography (HPLC) elution conditions, MS and MRM parameters, calibration standards) described in Lambert et al.[17]

Computational Methods. *Building Molecular Structures.* The molecular structures of the 49 more abundant molecules (Appendix 2 of the SI), monomer, and tetramer of PVP were built using the GaussView program.[22] The structures were built considering an environment at wine pH (3.5). In the case of anthocyanins, their flavylium ion and hydrated form have been considered. The geometries of these molecules were optimized at density functional theory (DFT) level[23] using the B3LYP method[24,25] with 6-31G(d,p) as basis set, which has been implemented in Gaussian 03 package program.[26]

In Silico Calculation of Interaction Energies. A semiempirical quantum mechanical strategy complemented with Monte Carlo conformational sampling[27−29] was used to calculate the interaction energy of molecule1−molecule2 complexes. In this case, the molecule1 represents the PVP tetramer, and the molecule2 represents each one of the 49 targets.

Molecular Dynamics Simulation (MDS). The polyvinylpyrrolidone (PVP) monomer was used to generate 50 PVP chains of 20, 30, and 40 monomers long using LEAP module of AmberTools software.[30] Subsequently, using PACKMOL software,[31] these 50 chains were randomly distributed within a virtual sphere of 45 Å radius centered in the origin 0, 0, 0 (axes X, Y, Z, respectively). The chains were separated one from each other by a distance of at least 3 Å. These steps generated a PVP spherical microparticle of 90 Å diameter with the aim of transforming this PVP microparticle to a PVPP microparticle (the highly cross-linked version of PVP). The LEAP module was used to perform the cross-linking procedure.[32] It is based on a cyclic iteration scheme, and each cycle consists of three steps: (1) random breaking of a pyrrolidone ring, (2) covalent bonding of the obtained COOH group to the nearest amino group (only if it is 5 Å away), and (3) minimization of the system performed with the steepest descent algorithm and the universal force field (UFF) using openbabel software.[33] The steps from 1 to 3 are repeated until 60% of the pyrrolidone rings are broken. The graphical scheme of the formation of the PVPP microparticle is shown in Appendix 3 of the SI.

The obtained PVPP microparticle was added in the center of a solvent box of the following sizes: 150, 150, and 150 Å (axes X, Y, and Z, respectively). Subsequently, the box was solvated considering a 90:10 mixture of water and ethanol with the aim of simulating the main components of rosé wine. The amounts of ethanol and water molecules (TIP3) were obtained on the basis of their corresponding molecular experimental density (0.789 g cm^{-3} for ethanol and 1 g cm^{-3} for water). Subsequently, the 30 polyphenols that had the best interaction energies (less than or equal to −2.7 kcal mol^{-1}, calculated with semiempirical methods) were added to the inside of the box (8 Å away from the surface of the PVPP microparticle). Finally, two MDS were run using the Desmond/Maestro software academic version 4.4[34] carried out in an NPT ensemble for about 50 ns. The first MDS considers the anthocyanins in their flavylium ion form, and the second MSD considers them in their hydrated form. The default relaxation protocol implemented in Desmond was used. The OPLS force field was applied to the system. From the results of the MDS, 1000 frames were extracted, which were analyzed using VMD 1.9.2 software.[35]

Statistical Analyses. All the experiments were carried out in triplicate (biological replicates). Statistical analyses, including means, standard deviations, and analysis of variance (ANOVA), were performed using Excel (Microsoft, Redmond, WA, USA).

RESULTS AND DISCUSSION

Effect of PVPP Treatment on Rosé Wine Colors. As expected, the CIELAB coordinates of the wines were modified by the PVPP treatment. The values of the different color coordinates measured on the control wines and after treatments are available as supplementary data together with the corresponding statistical analyses (Appendix 4 of the SI). The normalized average measures (in percentage compared to control wines) for all samples are reported in Figure 2.

DOI: 10.1021/acs.jafc.7b04461
J. Agric. Food Chem. XXXX, XXX, XXX−XXX

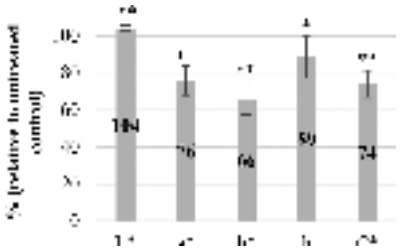

Figure 2. Average CIELAB coordinates measured in the six wines after PVPP treatment. Asterisks (*) and (**) on the tops of the bars indicate a significant difference with the control (Tukey (HSD): $p < 0.05$ and $p < 0.01$, respectively). Results are normalized to the untreated control (100%).

Lightness L* has increased by only 4% on average, which is a small change but statistically significant in all the wines. This limited rise can be explained by the fact that our wines had relatively high initial L* values.

The a* and b* coordinates, respectively, decreased by 24% and 34% on average for all the wines, which indicated a statistically significant reduction of the red and yellow color components, respectively. We can then assume that PVPP affected color-active polyphenols such as anthocyanins and their derivatives and flavonols. This color drop can be due to the reduction of these pigment concentrations but also to the reduction of the copigmentation effect because of the adsorption of copigments.[36−38] The yellow color measured by the b* coordinate may also be linked to oxidation phenomena which are very common in wines. PVPP may have removed orange pigments resulting from oxidation of compounds such as flavanols[3−6,39] or from reactions of anthocyanin pigments,[8−10] inducing a reduction of the b* value.

Logically, the C* parameter followed the same trend and decreased by 26%, reflecting a color intensity loss in the treated wines.

The h parameter also slightly decreased by 11%, which is the result of the b* component being more affected by PVPP than the a* one.

In all six wines, the ΔE value between the colors of the wines before and after PVPP fining is superior to 1 (Appendix 4 of the SI) meaning that a standard observer can see a difference in color. For two of the six wines, 3, $5 < \Delta E < 5$, so a clear difference in color is noticed. For the others, $\Delta E > 5$, so the observer notices two different colors.[21]

Mass Spectrometry Results. The polyphenol composition of the rosé wines was analyzed before and after treatment by PVPP by LC-MS/MS as previously described in Lambert et al.[17] The concentrations of the different compounds for all the wines (before and after treatment) are available as supplementary data (Appendix 5 of the SI).

For each molecule family, except for the alcohols and amino acids, the quantities in the treated wines are statically different from those measured in the initial wines according to the ANOVA analysis. However, the absorption capacity of rosé wine polyphenols to PVPP was very different from one family to another, confirming the existence of a very selective adsoption process (Figure 3). Three polyphenol families were the most affected by the PVPP treatment: flavonols, flavanols, and some anthocyanins, namely, coumaroylated anthocyanins.

Forty-two percent of the initial flavonols were adsorbed by PVPP. This is in accordance with the lower value of the CIELAB b* value after treatment. Flavonols are pale yellow pigments,[40] and a positive b* value stands for yellowish colors, so a smaller quantity of these molecules may have contributed to the reduction of the b* coordinate. It is also likely that orange pigments such as xanthylium derivatives,[6,7] not targeted in our LC-MRM-MS method, are removed by the treatment. Furthermore, flavonols are a family of molecules involved in copigmentation[36] that is responsible for color enhancement in the wines by increasing the red color of anthocyanins. A reduction of the concentration of these molecules would limit the copigmentation effect and induce a reduction of the wine color, leading to a lower a* value.

Concerning flavanols, 64% of their total content was adsorbed by PVPP, which represented the most impacted family of polyphenols on average for all the wines. Some important selectivity was observed within this group of polyphenols as adsorption increased with oligomerization. Indeed, trimers were slightly more adsorbed than dimers (79% vs 72%) and much more adsorbed than monomers

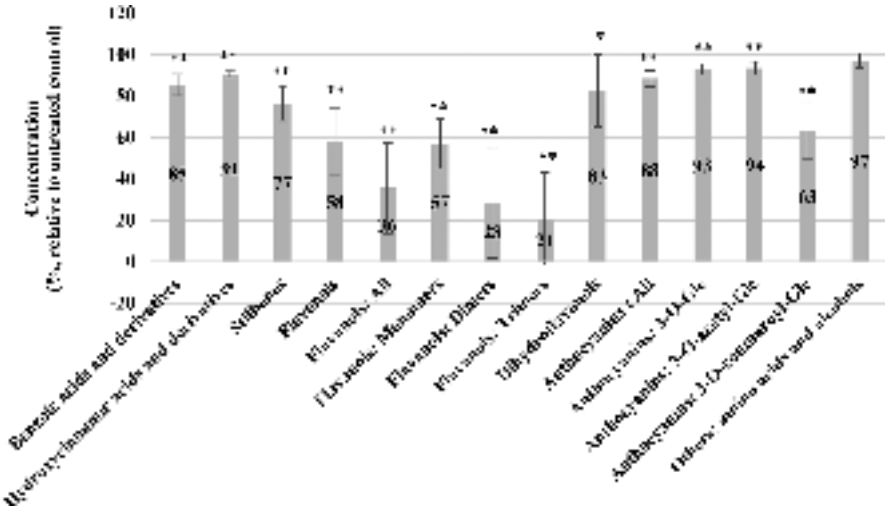

Figure 3. Average rosé wine polyphenols concentrations measured in the six wines after PVPP treatment. Asterisks (*) and (**) on the tops of the bars indicate a significant difference with the control (Tukey (HSD): $p < 0.05$ and $p < 0.01$, respectively). Results are normalized to the untreated control (100%).

DOI: 10.1021/acs.jafc.7b04461
J. Agric. Food Chem. XXXX, XXX, XXX−XXX

(43%). These results are in accordance with the study published by Mitchell et al.[41] where the authors showed that tendency of the proanthocyanidins to bind to PVPP increased with the degree of polymerization ((*n* = 3) > (*n* = 2) > (*n* = 1)). As the number of units increases, so does the number of hydroxyl groups and aromatic rings. This, respectively, implies more hydrogen-bonding sites and hydrophobic interactions, inducing a better PVPP affinity.[14,16] The same tendencies were also reported for binding of flavanols to different proteins and peptides, like salivary proteins, gelatins, casein, and poly-L-proline, and precipitation of the resulting complexes that increased significantly with the degree of polymerization of proanthocyanidins.[42−48]

PVPP did not remove an important proportion of anthocyanins with a mean adsorption capacity of 12% for all forms. However, the coumaroylated anthocyanins (anthocyanin-3-*O*-coumaroyl-Glc) showed a much higher affinity toward PVPP with a 37% average decrease. Although PVPP was previously reported to adsorb anthocyanins in wines,[49,50] this is the first time to our knowledge that such an affinity is described for coumaroylated anthocyanins. This type of acylated molecules with an additional phenol ring is less polar than other anthocyanins.[51] Thus, a stronger hydrophobic interaction might be responsible for this peculiar affinity.

The selective affinity of PVPP toward six phenolic compounds was already investigated by Durán-Lara et al.[52] They showed that PVPP exhibits a higher affinity for quercetin (flavonol) and catechin (flavanol: monomer), a moderate affinity for epicatechin (flavanol: monomer) and gallic acid (benzoic acid), and a lower affinity for 4-methycatechol (alcohol) and caffeic acid (hydroxycinnamic acid). This is in accordance with our results, where the affinity order for these different polyphenol families is as follows: flavanols (monomers) ≈ flavonols > benzoic acids > hydroxycinnamic acids > alcohols.

Computational Results. Structure based computational models were investigated to better understand the different affinities observed between PVPP and rosé wine polyphenols (results are shown in Table 1).

If we consider all components together, there is no correlation between the polyphenol adsorption percentage by PVPP and the calculated interaction energies. The corresponding graph is available as supplementary data (Appendix 6 of the SI).

However, correlation within the flavanol family was observed between the experimental adsorption and the calculated interaction energy (Appendix 7 of the SI). For flavanols, adsorption of trimers was higher than that of dimers that was higher than that of monomers. The same trend can be observed in the in-silico calculations: the best interaction energy is obtained for the trimers, followed by the dimers and, finally, the monomers (Table 1).

We can also observe that coumaroylated anthocyanins and other anthocyanins have very different behaviors. At wine pH, it is possible to find anthocyanins in their cationic form (A^+) and in greater proportion in their hydrated form (AOH). The latter form is due to nucleophilic attack of water on the flavylium ion of the anthocyanins. The anthocyanins under their hydrated form showed higher interaction energies than their flavylium ion form (Table 1). Also, when comparing these values with the experimental adsorption, an improvement in the correlation was obtained for anthocyanins in their hydrated form, with an r^2 higher than 0.9 (Appendix 7b of the SI).

Table 1. Adsorption Percentages and Interaction Energies Calculated at Semi-Empirical Quantum Mechanical Level

id	name	adsorption percentage	interaction energy kcal mol^{-1} (A^+/AOH)
1	gallic acid	17 ± 6	−2.473
2	protocatechuic acid	10 ± 3	−2.422
3	syringic acid	1 ± 7	−2.572
4	ethyl ester of gallic acid	41 ± 14	−2.473
5	caffeic acid	12 ± 9	−2.548
6	*cis*-caftaric acid	10 ± 2	−2.633
7	*trans*-caftaric acid		−2.642
8	fertaric acid	6 ± 8	−2.594
9	ferulic acid	66 ± 26	−2.580
10	*p*-coumaric acid	3 ± 19	−2.513
11	*cis*-coutaric acids	12 ± 20	−2.535
12	*trans*-coutaric acids		−2.601
13	caffeic acid ethyl ester	5 ± 22	−2.542
14	coumaric acid ethyl ester	12 ± 21	−2.515
15	2 *S*-glutathionyl caftaric acid GRP (grape reaction product)	8 ± 8	−3.380
16	*cis*-piceid	7 ± 22	−2.973
17	*trans*-piceid	33 ± 42	−2.965
18	*cis*-resveratrol	83 ± 15	−2.657
19	*trans*-resveratrol	20 ± 30	−2.663
20	quercetin glucuronide	44 ± 16	−2.955
21	myricetol glucuronide	19 ± 12	−3.194
22	(+)-catechin	45 ± 14	−2.772
23	dimer cat B1 (procyanidin B1)	72 ± 27	−3.223
24	dimer cat B2 (procyanidin B2)	66 ± 30	−3.107
25	dimer cat B3 (procyanidin B3)	81 ± 23	−3.187
26	(−)-epicatechin	38 ± 12	−2.822
27	trimer cat1 (procyanidin C1)	74 ± 35	−3.518
28	trimer cat2 (procyanidin C2)	80 ± 21	−3.392
29	astilbin	17 ± 18	−3.004
30	delphinidin 3-*O*-Glc	15 ± 6	(−3.201/−3.423)
31	malvidin 3-*O*-Glc	6 ± 3	(−3.201/−3.312)
32	peonidin 3-*O*-Glc	8 ± 2	(−3.213/−3.465)
33	petunidin 3-*O*-Glc	12 ± 4	(−3.221/−3.488)
34	cyanidin 3-*O*-acetyl-Glc	12 ± 4	(−3.290/−3.480)
35	delphinidin 3-*O*-acetyl-Glc	15 ± 7	(−3.210/−3.494)
36	malvidin 3-*O*-acetyl-Glc	6 ± 3	(−3.303/−3.412)
37	peonidin 3-*O*-acetyl-Glc	6 ± 3	(−3.178/−3.443)
38	petunidin 3-*O*-acetyl-Glc	11 ± 5	(−3.225/−3.426)
39	cyanidin 3-*O*-coumaroyl-Glc	62 ± 22	(−3.447/−3.911)
40	delphinidin 3-*O*-coumaroyl-Glc	60 ± 26	(−3.370/−3.937)
41	malvidin 3-*O*-coumaroyl-Glc	34 ± 13	(−3.467/−3.543)
42	peonidin 3-*O*-coumaroyl-Glc	44 ± 16	(−3.376/−3.892)
43	petunidin 3-*O*-coumaroyl-Glc	56 ± 30	(−3.413/−3.854)
44	*p*-hydroxyphenylpyranomalvidin-3-*O*-Glc	19 ± 21	(−3.297/−3.438)
45	carboxypyranomalvidin 3-*O*-Glc = vitisin A	13 ± 18	(−3.344/−3.432)
46	tryptophan	14 ± 8	−2.793
47	tryptophol	3 ± 14	−2.481
48	tyrosine	2 ± 3	−2.574
49	tyrosol	2 ± 3	−2.237

All-atom MDS were performed in order to understand the molecular behavior between PVPP polymer and the 30 polyphenols that had the best interaction energies (Table 1) immersed in a solvent box that simulates the main components of the rosé wine (ethanol/water). Figure 4a shows the initial

DOI: 10.1021/acs.jafc.7b04461
J. Agric. Food Chem. XXXX, XXX, XXX−XXX

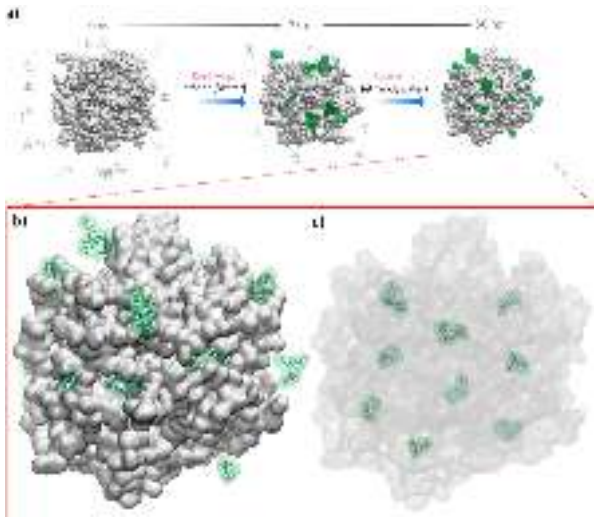

Figure 4. Snapshots of MDS stages. (a) The initial state of PVPP–polyphenols system and their behavior at 25 and 50 ns. The polyphenols colored green are those that have been captured by PVPP, both in (b) the micropockets of the surface and in (c) their interior cavities.

state of PVPP–polyphenols system, and its behavior at 25 and 50 ns. The polyphenols colored with green are those that have been captured by PVPP. The PVPP microparticle has micropockets on the surface, which allow the interaction and capture of large polyphenols, such as anthocyanins and flavanols (dimers and trimers) (Figure 4b). The PVPP porous structure generates small cavities capable of capturing and retaining the smaller polyphenols (Figure 4c).

The studies with molecular simulation allowed observing the binding interactions that govern the affinity of PVPP for flavanols and coumaroyl anthocyanins, focusing on six polyphenols with great absorption capacity: procyanidin B1, procyanidin B2, procyanidin B3, procyanidin C1, procyanidin C2, and cyanidin-3-*O*-coumaroyl-Glc (Figure 5). Catechin and epicatechin were incorporated into the analysis by way of comparison. There is a presence of characteristic hydrogen bonds in all studied systems, the difference being in the number of bonds and their stability throughout the simulation (Appendix 8 of the SI). The catechin and epicatechin monomers (Figure 5a, e) can form only between one and two hydrogen bonds mainly with the regions of PVPP internal cavities, whereas their dimers, trimers, and cyanidin-3-*O*-coumaroyl-Glc can form between two and four hydrogen bonds (Appendix 8 of the SI) in the surface pockets of the PVPP particle (Figure 5b–d, f–h). Comparing the dimers and trimers of flavanols with the cyanidin-3-*O*-coumaroyl-Glc, it can be observed that hydrophobic interactions play an important role in their differentiation. The trimers are able to generate more π-alkyl type interactions between their aromatic rings and the PVPP backbone; this could enhance the affinity for the polymer, improving the absorption capacity of PVPP.

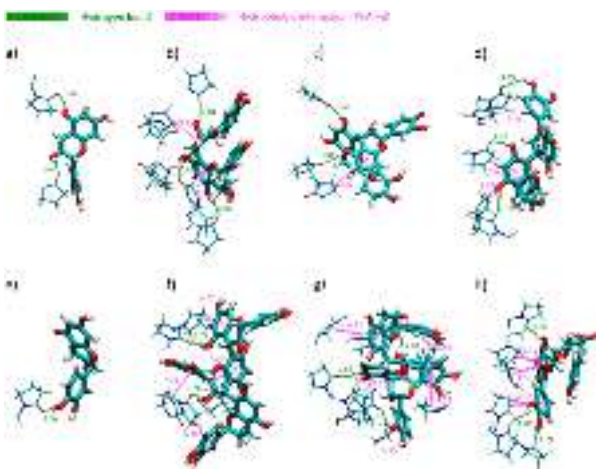

Figure 5. Snapshots of PVPP–polyphenols binding interactions. These are the polyphenols with greater absorption capacity for the flavanols and anthocyanins families: (a) catechin, (b) procyanidin B1, (c) procyanidin B2, (d) procyanidin B3, (e) epicatechin, (f) procyanidin C1, (g) procyanidin C2, and (h) canidin-3-*O*-coumaroyl-Glc.

As discussed previously, the anthocyanins in their hydrated form showed higher interaction energies, compared to their flavylium ion form, and a strong correlation with adsorption percentage was evidenced. Anthocyanins in their hydrated form showed a better affinity for PVPP mainly because of the presence of hydrogen bonds that remained stable for more than 80% of the simulation time (Appendix 9 of the SI). These computationally studied models would indicate that the hydrated structures of the anthocyanins are the preferred forms for adsorption of phenolic compounds by PVPP.

Altogether, our results showed the high selectivity for the polyphenol adsorption in the process of treating rosé wines by PVPP. Further research is needed to include other polyphenols involved such as tannin-anthocyanin adducts or oxidized forms of polyphenols.

■ ASSOCIATED CONTENT

Supporting Information

The Supporting Information is available free of charge on the ACS Publications website at DOI: 10.1021/acs.jafc.7b04461.

Appendix 1. Evolution of CIEL*a*b* parameters of two wines exposed to PVPP for 7 h and statistics associated (Tukey (HSD): $p < 0.05$). Appendix 2. Structures of the 49 targets considering their protonation state at the wine pH. Appendix 3. Methodology for design and study by SDM of the intermolecular properties of PVPP–polyphenols system. Appendix 4. Complete L*a*b* results. Appendix 5. Complete UPLC-QqQ-MS results: concentrations before (C) and after treatment (PVPP) (mean ± standard deviation, $n = 3$). Appendix 6. Correlation between PVPP/polyphenols interaction energy calculations (kcal mol^{-1}) and adsorption percentage measured in rosé wines for all the polyphenols. Appendix 7. Correlation between PVPP/polyphenols interaction energy calculations (kcal mol^{-1}) and adsorption percentage measured in rosé wines for flavanols and anthocyanins. Appendix 8. Number of hydrogen bonds between PVPP and polyphenols with better affinity: flavanols (monomers, dimers, trimers) and cyanidin-3-*O*-coumaroyl-Glc. Appendix 9. Comparative graphs of the number of hydrogen bonds between PVPP and the five coumaroylated anthocyanins considering (a) their flavylium ion form and (b) their hydrated form (DOCX)

DOI: 10.1021/acs.jafc.7b04461
J. Agric. Food Chem. XXXX, XXX, XXX–XXX

AUTHOR INFORMATION

Corresponding Author

*Tel.: +33411759567. Fax: +33411759638. E-mail: cedric.saucier@umontpellier.fr.

ORCID

Leonardo S. Santos: 0000-0002-1697-4200

Cédric Saucier: 0000-0001-6677-4488

Funding

The authors would like to thank the Biolaffort Company for funding. Fabian Avila-Salas is grateful for the Postdoctoral Fondecyt grant 3170909.

Notes

The authors declare no competing financial interest.

ACKNOWLEDGMENTS

The authors would like to thank Arnaud VERBAERE for having taken part in the experimentations.

REFERENCES

(1) Cheynier, V.; Dueñas-Paton, M.; Salas, E.; Maury, C.; Souquet, J.-M.; Sarni-Manchado, P.; Fulcrand, H. Structure and Properties of Wine Pigments and Tannins. *Am. J. Enol. Vitic.* **2006**, *57*, 298−305.

(2) Saucier, C. T.; Waterhouse, A. L. Synergetic activity of catechin and other antioxidants. *J. Agric. Food Chem.* **1999**, *47*, 4491−4494.

(3) Simpson, R. F. Factors affecting oxidative browning of white wine. *VITIS* **1982**, *21*, 233−239.

(4) Cheynier, V.; Rigaud, J.; Souquet, J. M.; Barillere, J. M.; Moutounet, M. Effect of pomace contact and hyperoxidation on the phenolic composition and quality of Grenache and Chardonnay wines. *Am. J. Enol. Vitic.* **1989**, *40*, 36−42.

(5) Oliveira, C. M.; Silva Ferreira, A. C.; De Freitas, V.; Silva, A. M. S. Oxidation mechanisms occurring in wines. *Food Res. Int.* **2011**, *44*, 1115−1126.

(6) Es-Safi, N. E.; Guernevé, C.; Fulcrand, H.; Cheynier, V.; Moutounet, M. Xanthylium salts formation involved in wine colour changes. *Int. J. Food Sci. Technol.* **2000**, *35*, 63−74.

(7) George, N.; Clark, A. C.; Prenzler, P. D.; Scollary, G. R. Factors influencing the production and stability of xanthylium cation pigments in a model white wine system. *Aust. J. Grape Wine Res.* **2006**, *12*, 57−68.

(8) Sarni-Manchado, P.; Fulcrand, H.; Souquet, J.-M.; Cheynier, V.; Moutounet, M. Stability and color of unreported wine anthocyanin-derived pigments. *J. Food Sci.* **1996**, *61*, 938−941.

(9) De Freitas, V.; Mateus, N. Formation of pyranoanthocyanins in red wines: a new and diverse class of anthocyanin derivatives. *Anal. Bioanal. Chem.* **2011**, *401*, 1463−1473.

(10) Vallverdú-Queralt, A.; Biler, M.; Meudec, E.; Le Guernevé, C.; Vernhet, A.; Mazauric, J.-P.; Legras, J.-L.; Loonis, M.; Trouillas, P.; Cheynier, V.; Dangles, O. p-Hydroxyphenyl-pyranoanthocyanins: an experimental and theoretical investigation of their acid-base properties and molecular interactions. *Int. J. Mol. Sci.* **2016**, *17*, 1842.

(11) Nikolantonaki, M.; Magiatis, P.; Waterhouse, A. L. Measuring protection of aromatic wine thiols from oxidation by competitive reactions vs wine preservatives with ortho-quinones. *Food Chem.* **2014**, *163*, 61−67.

(12) Doner, L. W.; Bécard, G.; Irwin, P. L. Binding of Flavonoids by Polyvinylpolypyrrolidone. *J. Agric. Food Chem.* **1993**, *41*, 753−757.

(13) McMurrough, I.; Madigan, D.; Smytht, M. R. Adsorption by Polyvinylpolypyrrolidone of Catechins and Proanthocyanidins from Beer. *J. Agric. Food Chem.* **1995**, *43*, 2687−2691.

(14) Magalhães, P. J.; Vieira, J. S.; Goncalves, L. M.; Pacheco, J. G.; Guido, L. F.; Barros, A. A. Isolation of phenolic compounds from hop extracts using polyvinylpolypyrrolidone: Characterization by high-performance liquid chromatography−diode array detection−electro-spray tandem mass spectrometry. *J. Chromatogr. A* **2010**, *1217*, 3258−3268.

(15) Rehmanji, M.; Gopal, C.; Mola, A. Beer Stabilization Technology-Clearly a Matter of Choice. *Master Brew. Assoc. Am.* **2005**, *42*, 332−338.

(16) Laborde, B.; Moine Ledoux, V.; Richard, T.; Saucier, C.; Dubourdieu, D.; Monti, J. P. PVPP-polyphenol complexes: A molecular approach. *J. Agric. Food Chem.* **2006**, *54*, 4383−4389.

(17) Lambert, M.; Meudec, E.; Verbaere, A.; Mazerolles, G.; Wirth, J.; Masson, G.; Cheynier, V.; Sommerer, N. A High-Throughput UHPLC-QqQ-MS Method for Polyphenol Profiling in Rosé wines. *Molecules* **2015**, *20*, 7890−7914.

(18) CIE, CIE 1976 L*a*b* Colour Space, ISO 11664−4:2008 (CIE S 014−4/E: 2007).

(19) Hernández, B.; Sáenz, C.; Alberdi, C.; Alfonso, S.; Diñeiro, J. M. Colour Evolution of Rosé Wines after Bottling. *S. Afr. J. Enol. Vitic.* **2011**, *32*, 42−50.

(20) Korifi, R.; LeDréau, Y.; Antinelli, J.-F.; Valls, R.; Dupuy, N. CIEL*a*b* color space predictive models for colorimetry devices−Analysis of perfume quality. *Talanta* **2013**, *104*, 58−66.

(21) Mokrzycki, W. S.; Tatol, M. Color difference ΔE − A survey. *Mach. Graph. Vis.* **2011**, *20*, 383−411.

(22) Dennington, R., II; Keith, T.; Milliam, J.; Eppinnett, K.; Hovell, W. L.; Gilliland, R. *GaussView*, version 3.09; Semichem, Inc.: Shawnee Mission, KS, 2003.

(23) Andzelm, J.; Wimmer, E. Density functional gaussian-type-orbital approach to molecular geometries, vibrations, and reaction energies. *J. Chem. Phys.* **1992**, *96*, 1280−1303.

(24) Becke, A. D. Density-functional thermochemistry 0.5. Systematic optimization of exchange-correlation functionals. *J. Chem. Phys.* **1997**, *107*, 8554−8560.

(25) Lee, C. T.; Yang, W. T.; Parr, R. G. Development of the Colle-Salvetti correlation-energy formula into a functional of the electron-density. *Phys. Rev. B: Condens. Matter Mater. Phys.* **1988**, *37*, 785−789.

(26) Frisch, M. J.; Trucks, G. W.; Schlegel, H. B.; Scuseria, G. E.; Robb, M. A.; Cheeseman, J. R.; Montgomery, J. A., Jr.; Vreven, T.; Kudin, K. N.; Burant, J. C. *Gaussian 03*, revision C.02; Gaussian, Inc.: Wallingford, CT, 2004.

(27) Avila-Salas, F.; Sandoval, C.; Caballero, J.; Guinez-Molinos, S.; Santos, L. S.; Cachau, R. E.; Gonzalez-Nilo, F. D. Study of Interaction Energies between PAMAM Dendrimer and non-Steroidal Anti-Inflammatory Drug Using a Distributed Computational Strategy and Experimental Analysis by ESI-MS/MS. *J. Phys. Chem. B* **2012**, *116*, 2031−2039.

(28) Metropolis, N.; Rosenbluth, A. W.; Rosenbluth, M. N.; Teller, A. H.; Teller, E. Equation of State Calculations by Fast Computing Machines. *J. Chem. Phys.* **1953**, *21*, 1087−109.

(29) Fan, C. F.; Olafson, B. D.; Bladnco, M. Application of Molecular Simulation To Derive Phase Diagrams of Binary Mixtures. *Macromolecules* **1992**, *25*, 3667−3676.

(30) Wang, J.; Wolf, R. M.; Caldwell, J. W.; Kollman, P. A.; Case, D. A. Development and Testing of a General Amber Force Field. *J. Comput. Chem.* **2004**, *25*, 1157−1173.

(31) Martínez, L.; Andrade, R.; Birgin, E. G.; Martínez, J. M. (2009). PACKMOL: A package for building initial configurations for molecular dynamics simulations. *J. Comput. Chem.* **2009**, *30*, 2157−2164.

(32) Yin, M.; Ye, Y.; Sun, M.; Kang, N.; Yang, W. Facile Facile one-pot synthesis of a polyvinylpyrrolidone-based self-crosslinked fluorescent film. *Macromol. Rapid Commun.* **2013**, *34*, 616−620.

(33) O'Boyle, N. M.; Banck, M.; James, C. A.; Morley, C.; Vandermeersch, T.; Hutchison, G. R. Open Babel: An Open Chemical Toolbox. *J. Cheminf.* **2011**, *3*, 33.

(34) D. E. Shaw Research. *Desmond Molecular Dynamics System*, version 3.4; New York, 2013.

(35) Humphrey, W.; Dalke, A.; Schulten, K. VMD: Visual Molecular Dynamics. *J. Mol. Graphics* **1996**, *14*, 33−38.

(36) Boulton, R. The copigmentation of anthocyanins and its role in the color of red wine: a critical review. *Am. J. Enol. Viticult.* **2001**, *52*, 67−87.

DOI: 10.1021/acs.jafc.7b04461
J. Agric. Food Chem. XXXX, XXX, XXX−XXX

(37) Gutiérrez, I. H.; Lorenzo, E. S. P.; Espinosa, A. V. Phenolic composition and magnitude of copigmentation in young and shortly aged red wines made from the cultivars, Cabernet Sauvignon, Cencibel, and Syrah. *Food Chem.* **2005**, *92*, 269−283.
(38) Mirabel, M.; Saucier, C.; Guerra, C.; Glories, Y. Copigmentation in model wine solutions: Occurrence and relation to wine aging. *Am. J. Enol. Viticult.* **1999**, *50*, 211−218.
(39) Guyot, S.; Vercauteren, J.; Cheynier, V. Structural determination of colourless and yellow dimers resulting from (+)-catechin coupling catalyzed by grape polyphenoloxidase. *Phytochemistry* **1996**, *42*, 1279−1288.
(40) Jeffery, D. W.; Parker, M.; Smith, P. A. Flavonol composition of Australian red and white wines determined by high-performance liquid chromatography. *Aust. J. Grape Wine Res.* **2008**, *14*, 153−161.
(41) Mitchell, A. E.; Hong, Y.-J.; May, J. C.; Wright, C. A.; Bamforth, C. W. A Comparison of Polyvinylpolypyrrolidone (PVPP), Silica Xerogel and a Polyvinylpyrrolidone (PVP)−Silica Co-Product for Their Ability to Remove Polyphenols from Beer. *J. Inst. Brew.* **2005**, *111* (1), 20−25.
(42) Baxter, N. J.; Lilley, T. H.; Haslam, E.; Williamson, M. P. Multiple interactions between polyphenols and a salivary proline-rich protein repeat result in complexation and precipitation. *Biochemistry* **1997**, *36*, 5566−5577.
(43) Sarni-Manchado, P.; Cheynier, V. Study of non-covalent complexation between catechin derivatives and peptides by electrospray ionization mass spectrometry. *J. Mass Spectrom.* **2002**, *37*, 609−616.
(44) Canon, F.; Giuliani, A.; Paté, F.; Sarni-Manchado, P. Ability of a salivary intrinsically unstructured protein to bind different tannin targets revealed by mass spectrometry. *Anal. Bioanal. Chem.* **2010**, *398*, 815−822.
(45) Okuda, T.; Mori, K.; Hatano, T. Relationship of the structures of tannins to the binding activities with hemoglobin and methylene blue. *Chem. Pharm. Bull.* **1985**, *33*, 1424−1433.
(46) Kumar, R.; Horigome, T. Fractionation, characterization and protein-precipitating capacity of the condensed tannins from Robinia pseudoacacia L. leaves. *J. Agric. Food Chem.* **1986**, *34*, 487−489.
(47) Ricardo-da-Silva, J. M.; Cheynier, V.; Souquet, J.-M.; Moutounet, M. Interaction of grape seed procyanidins with various proteins in relation to wine fining. *J. Sci. Food Agric.* **1991**, *57*, 111−125.
(48) Maury, C.; Sarni-Manchado, P.; Lefebvre, S.; Cheynier, V.; Moutounet, M. Influence of fining with different molecular weight gelatins on proanthocyanidin composition and perception of wines. *Am. J. Enol. Vitic.* **2001**, *52*, 140−145.
(49) Castillo-Sánchez, J. X.; García-Falcón, M. S.; Garrido, J.; Martínez-Carballo, E.; Martins-Dias, L. R.; Mejuto, X. C. Phenolic compounds and colour stability of Vinhao wines: Influence of wine-making protocol and fining agents. *Food Chem.* **2008**, *106*, 18−26.
(50) Hornsey, I. Clarification, stabilization and preservation. *The Chemistry and Biology of Winemaking*; Royal Society of Chemistry: Cambridge, U. K., 2007; Chapter 6, pp 242−292.
(51) Escribano-Bailon, T.; Santos-Buelga, C.; Rivas-Gonzalo, J. C. Anthocyanins in cereals. *J. Chromatogr. A* **2004**, *1054*, 129−141.
(52) Durán-Lara, E. F.; López-Cortés, X. A.; Castro, R. I.; Avila-Salas, F.; González-Nilo, F. D.; Laurie, V. F.; Santos, L. S. Experimental and theoretical binding affinity between polyvinylpolypyrrolidone and selected phenolic compounds from food matrices. *Food Chem.* **2015**, *168*, 464−470.

DOI: 10.1021/acs.jafc.7b04461
J. Agric. Food Chem. XXXX, XXX, XXX−XXX